Electronic properties of $Ca_2CuO_2Cl_2$ and $Ca_2CuO_2Br_2$

L. F. Mattheiss

AT&T Bell Laboratories, Murray Hill, New Jersey 07974

(Received 29 January 1990)

The linear augmented-plane-wave method has been applied to calculate the electronic band properties of the halo-oxocuprates $Ca_2CuO_2Cl_2$ and $Ca_2CuO_2Br_2$, a class of quaternaries that form with the same K_2NiF_4-type structure as La_2CuO_4. The results exhibit the same generic features that characterize previous cuprate superconductor parent compounds such as La_2CuO_4, including a single half-filled Cu $d(x^2-y^2)$–O $p(x,y)$ σ-antibonding subband at E_F. A tight-binding analysis shows that the qualitative differences between the valence-band results at lower energies for the halo-oxocuprates and La_2CuO_4 are due to the increased binding energies [relative to Cu(3d)] of the Br(4p) (~ 0.5 eV) and Cl(3p) (~ 1.3 eV) states as compared with the apical O(2p) (~ 0.1 eV) states.

As shown by the early studies of Grande and Müller-Buschbaum,[1] the halo-oxocuprates with the general formula $M_2CuO_2X_2$ (M = Ca, Sr; X = Cl, Br) represent an interesting structural and chemical analog to La_2CuO_4, the parent compound involved in the Bednorz-Müller discovery[2] of high-T_c superconductivity in the La-Ba-Cu-O ($T_c \approx 30$ K) system. Both classes of compounds share the same K_2NiF_4-type structure[1,3] and contain CuO_2 planes with short (~ 1.9–2.0 Å) Cu-O bond distances. The main difference is that, in the halo-oxocuprates, the apical oxygens are replaced by Cl or Br at somewhat larger (~ 2.7–3.0 Å versus ~ 2.4 Å) bond distances (See Fig. 1).

Based on these structural similarities as well as simple valence considerations, one can expect these $M_2CuO_2X_2$ halo-oxocuprates to possess the same planar Cu $d(x^2-y^2)$–O $p(x,y)$ σ-antibonding subband[4] that is half-filled in undoped La_2CuO_4 and represents the familiar characteristic feature of high-T_c cuprate superconductors. This suggests that substitutional doping of monovalent or trivalent elements for the alkaline-earth constituents (i.e., $Ca_{2-x}K_xCuO_2Cl_2$, $Ca_{2-x}La_xCuO_2Cl_2$, etc.) will alter the band filling within the CuO_2 planes, thereby producing metallic properties as well as possible high-temperature superconductivity. The results of recent studies[5,6] on $Sr_{2-x}M_xCuO_2Cl_2$ (M = Na, K vacancy) contain both encouraging and discouraging news. The encouraging news is that long-range antiferromagnetic order has been observed[5] in the $Sr_2CuO_2Cl_2$ parent compound, with a Cu spin alignment which is similar to that found in La_2CuO_4. The bad news is that efforts to drive the system metallic and superconducting by either hole or electron doping have been unsuccessful thus far.[6]

Previous attempts to synthesize high-T_c halo-oxocuprates have produced mixed results. The earliest studies focused on efforts to incorporate fluorine into the 95-K superconductor,[7] $YBa_2Cu_3O_7$. Although superconductivity at 155 K has been reported[8] in a multiphase sample with nominal composition $YBa_2Cu_3F_2O_y$, numerous other groups[9] have failed to reproduce this result. However, more recent thin-film studies[10] have

shown that fluorination or chlorination can stabilize a new 80-K superconducting phase, $YBa_2Cu_4O_8$, though no evidence of halogen doping was detected in the superconducting phase. Recently, James, Zahurak, and Murphy[11] have shown that fluorine-doped $Nd_2CuO_{3.7}F_{0.3}$ samples are n-type conductors at room temperature and exhibit bulk superconductivity below ~ 27 K.

The purpose of the present investigation is to evaluate the electronic properties of two representative halo-oxocuprates, $Ca_2CuO_2Cl_2$ and $Ca_2CaO_2Br_2$, in order to assess their parental possibilities as high-temperature superconductors. With this objective, the self-consistent electronic band structures of $Ca_2CuO_2Cl_2$ and $Ca_2CuO_2Br_2$ have been calculated in the local-density approximation with the use of the linear augmented-plane-wave (LAPW) method.[12] The implementation imposes no shape approximations on either the charge density or
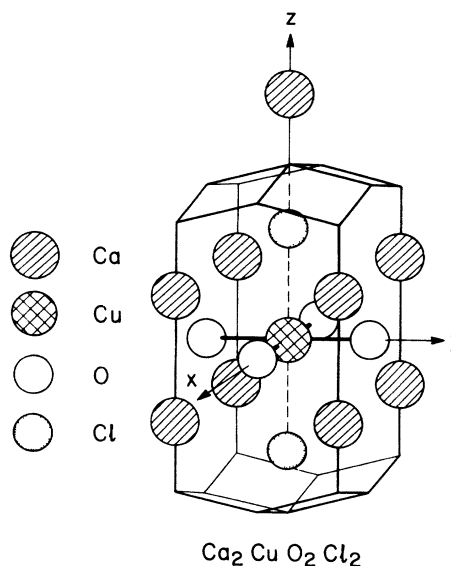

$Ca_2 Cu O_2 Cl_2$

FIG. 1. Primitive unit cell for bct $Ca_2CuO_2Cl_2$.

the potential. The calculations incorporate a LAPW basis that includes plane waves with an 11-Ry cutoff (~470–540 LAPW's) and spherical-harmonic terms through $l = 8$. The charge density and potential are expanded using ~7000 plane waves (64 Ry) in the interstitial region and lattice-harmonic expansions ($l_{max} = 6$) within the muffin-tin spheres. The Brillouin-zone integrations have been carried out with the use of a 12-point k mesh in the irreducible wedge of the body-centered-tetragonal (bct) zone. Exchange and correlation effects have been treated with the use of the Wigner interpolation formula.[13]

The present calculations are based on the structural parameters that were determined from x-ray -diffraction studies by Grande and Müller-Buschbaum.[1] The primitive unit cell for bct $Ca_2CuO_2Cl_2$ (space group $I4/mmm$) is shown in Fig. 1. For $Ca_2CuO_2Cl_2$ ($Ca_2CuO_2Br_2$), the measured lattice parameters are $a = 3.87$ Å (3.88 Å) and $c = 15.0$ Å (17.3 Å), while the corresponding atom position parameters are $z(Ca) = 0.395$ (0.408) and $z(Cl) = 0.182$ [$z(Br) = 0.171$], respectively. The radii of the Cu (~1.05 Å) and O (~0.88 Å) muffin-tin spheres have been chosen so that they are nearly touching along the nearest-neighbor bond directions in the basal plane. In the present calculations, the atomic $Ca(4s^2)$, $Cu(3d^{10}4s^1)$, $O(2s^22p^4)$, and $Cl(3s^23p^5)$ or $Br(4s^24p^5)$ states are treated as valence electrons whereas the more tightly bound corelike levels are taken into account with the use of a frozen-core approximation.[12]

The LAPW band-structure results for $Ca_2CuO_2Cl_2$ and $Ca_2CuO_2Br_2$ are plotted along selected symmetry lines in the basal plane of the bct Brillouin zone in Fig. 2. The nearly filled valence-band manifold includes the 17 bands that evolve from the $Cu(3d)$, $O(2p)$, and $Cl(3p)$ or $Br(4p)$ atomic levels. The unoccupied conduction bands above ~3 eV represent the lowest portions of the $Cu(4s)$, $Ca(4s)$, and $Ca(3d)$ bands. Though not shown, additional low-energy valence-band states for $Ca_2CuO_2Cl_2$ ($Ca_2CuO_2Br_2$) include the $Cl(3s)$ [$Br(4s)$] corelike levels at ~ -15.0 eV (-14.5 eV) and the $O(2s)$ states at ~ -17.3 eV (-17.2 eV). The small calculated $Cl(3s)$-$Br(4s)$ energy shift reflects the 0.4-eV difference between the calculated atomic energies of the $Cl(3s)$ and $Br(4s)$ levels.

The valence-band results for $Ca_2CuO_2Cl_2$ and $Ca_2CuO_2Br_2$ are qualitatively similar to each other as well as to previous results[4] for La_2CuO_4. In each material, the valence bands are strongly two dimensional, exhibiting minimal dispersion (~0.1 eV) along the c axis near E_F. While the majority of the energy-band states in Fig. 2 are represented by solid circles, two band types of special interest are distinguished by means of square and triangular symbols, respectively. The squares identify the σ-type bonding and antibonding combinations of $Cu\,d(x^2-y^2)$ $-O\,p(x,y)$ orbitals that produce the familiar half-filled antibonding subband at E_F. Similarly, the triangles label LAPW states with predominant $Cl(3p)$ or $Br(4p)$ character within the corresponding muffin-tin
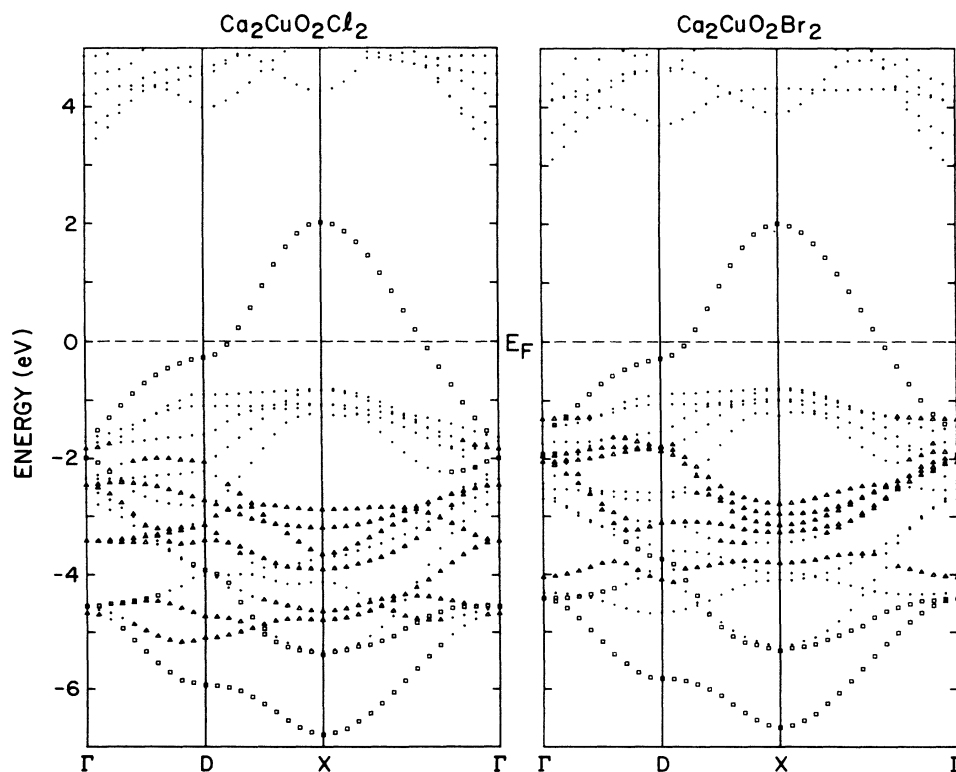

FIG. 2. LAPW energy-band results for (a) $Ca_2CuO_2Cl_2$ and (b) $Ca_2CuO_2Br_2$ plotted along basal-plane symmetry lines in the bct Brillouin zone, where $D = (\pi/a,0,0)$ and $X = (\pi/a,\pi/a,0)$, respectively. The squares (triangles) identify bands that have at least 30% $Cu\,d(x^2-y^2)$-$O\,p(x,y)$ [Cl or $Br\,p(x,y,z)$] orbital weight within the corresponding muffin-tin spheres.

spheres.

It is clear from Fig. 2 that the approximate degeneracy between the O(2p) and Cu(3d) levels in the La_2CuO_4 results[4] is now expanded to include the Cl(3p) and Br(4p) states in the halo-oxocuprates. However, there are some indications that the Br(4p)- and Cl(3p)-derived states occur at somewhat higher binding energies within the valence-band manifold. This is particularly evident in the band distribution near X, where five subbands with energy ~ -1 eV are split off from the lower-lying bands. These split-off bands include four states with predominant Cu(3d) character as well as a weakly admixed O$p(x,y)\pi$-antibonding state.

These general features of the $Ca_2CuO_2Cl_2$ and $Ca_2CuO_2Br_2$ energy bands are also reflected in the density-of-states (DOS) results which are shown in Fig. 3. These have been calculated with the use of tetrahedral interpolation involving LAPW results at 63 points in the bct irreducible Brillouin-zone wedge. The energy distribution of the Cu, O_2, and Cl_2 or Br_2 components of the muffin-tin-projected DOS result are surprisingly uniform, considering the electronegativity differences of the constituents. There is a slight tendency for the Cu(3d) DOS component in $Ca_2CuO_2Cl_2$ to peak near the upper valence-band energy range, thus suggesting a slightly larger Cu(3d)-Cl(3p) orbital-energy difference in this material. This effect is somewhat diminished in the corresponding Br compound.

As expected from previous results[4] for La_2CuO_4, the Ca DOS component is relatively small in both materials,
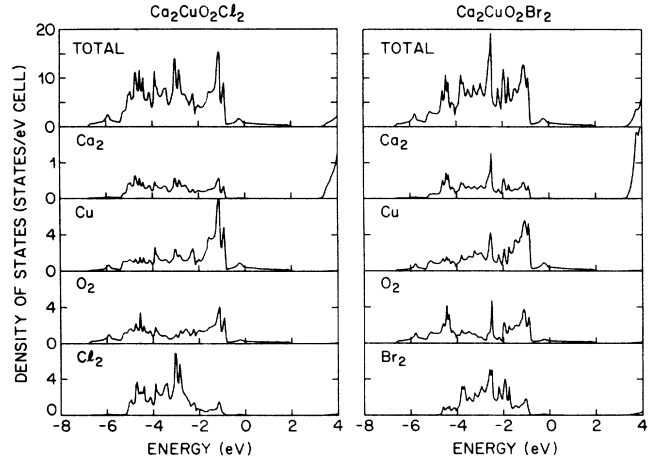

FIG. 3. Total and muffin-tin-projected LAPW density-of-states results for (a) $Ca_2CuO_2Cl_2$ and (b) $Ca_2CuO_2Br_2$, respectively.

particularly near the Fermi level, $E_F = 0$. In fact, at least part of this Ca DOS component is due to the "tails" of the O(2p) orbitals which extend into the relatively large ($R \approx 1.48$ Å) Ca muffin-tin spheres. Thus, Ca is a chemically inactive constituent with a formal valence of essentially +2. As in the case of La_2CuO_4, this suggests that substitutional doping with monovalent or trivalent elements at this site would represent the optimal procedure

TABLE I. Tight-binding parameters for $Ca_2CuO_2Cl_2$, $Ca_2CuO_2Br_2$, and La_2CuO_4, as determined from fits to LAPW results at Γ, D, X, and Z. Nearest-neighbor O-O interactions are treated in a modified two-center approximation, as discussed in the text.

Parameter	$Ca_2CuO_2Cl_2$ Sites [d(Å)]	Value (eV)	$Ca_2CuO_2Br_2$ Sites [d(Å)]	Value (eV)	La_2CuO_4 Sites [d(Å)]	Value (eV)
$E_{d(3z^2-r^2)}$	Cu	−2.025	Cu	−2.248	Cu	−2.351
$E_{d(x^2-y^2)}$		−2.031		−2.014		−2.447
$E_{d(xy)}$		−2.697		−2.617		−3.207
$E_{d(xz,yz)}$		−2.218		−2.229		−2.534
$E_{p\sigma}$	O	−3.683	O	−3.580	O	−3.965
$E_{p\pi}$		−2.657		−2.623		−3.112
E_{xy}	Cl	−3.446	Br	−2.764	O	−2.617
E_z		−3.805		−2.954		−2.835
$(pd\sigma)_1$	Cu-O	−1.422	Cu-O	−1.402	Cu-O	−1.525
$(pd\pi)_1$	[1.935]	0.719	[1.940]	0.678	[1.895]	0.754
$(pd\sigma)_2$	Cu-Cl	−0.553	Cu-Br	−0.608	Cu-O	−0.831
$(pd\pi)_2$	[2.730]	0.140	[2.946]	−0.189	[2.404]	0.270
$(pp\sigma)_1^s$	O-O	1.018	O-O	0.992	O-O	1.180
$(pp\sigma)_1^p$	[2.737]	0.578	[2.744]	0.605	[2.680]	0.528
$(pp\pi)_1$		−0.086		−0.098		0.024
$(pp\sigma)_2$	O-Cl	0.430	O-Br	0.466	O-O	0.446
$(pp\pi)_2$	[3.346]	0.023	[3.528]	0.000	[3.061]	0.019
$(pp\sigma)_3$	Cl-Cl	0.492	Br-Br	0.386	O-O	0.356
$(pp\pi)_3$	[3.413]	−0.077	[3.883]	−0.066	[3.226]	−0.048
$(pp\sigma)_4$	Cl-Cl	0.242	Br-Br	0.375	O-O	−0.028
$(pp\pi)_4$	[3.870]	−0.027	[3.880]	−0.043	[3.790]	−0.008
rms error		0.15		0.15		0.23

for adjusting the band filling within the CuO_2 planes. As is well known, this contributes the additional carriers (holes or electrons) which are generally believed to provide the superconducting carriers in the cuprate family of compounds.

It is evident that both the Cl and Br DOS components are essentially zero near E_F in Fig. 3. This feature, which is more prominent than the slightly reduced DOS exhibited[4] by the apical O_2 states in La_2CuO_4, implies that doping via halide vacancies or appropriate chemical substitutions at this site could provide an alternate means for adjusting the band filling within the $Cu d(x^2-y^2)$ $-O p(x,y)$ subband. This approach would be analogous to that proposed[11] for fluorine-doped $Nd_2CuO_{4-x}F_x$, where the fluorine dopants are believed to replace the Nd-coordinated oxygens in the T' structure at sites which are analogous to the apical oxygens (halogens) in La_2CuO_4 $(M_2CuO_2X_2)$.

Photoemission studies[14] have provided the first empirical information regarding the valence bandwidth and the relative binding energies of the $O(2p)$ and $Cl(3p)$ components in the closely related compound, $Sr_2CuO_2Cl_2$. According to these results, the measured valence bandwidth (~ 8 eV) is about 1–2 eV larger than the calculated value for $Ca_2CuO_2Cl_2$. A $Cl(3p)$-derived emission peak is observed at ~ -5.5 eV, somewhat below (~ 2 eV) that predicted by the DOS results of Fig. 3. In general, these discrepancies are similar to those observed in the earliest photoemission studies on Ba- and Sr-doped La_2CuO_4 and related cuprate superconductors.[15]

In order to provide a more detailed understanding of the electronic properties of the halo-oxocuprates $Ca_2CuO_2Cl_2$ and $Ca_2CuO_2Br_2$ and their relationship to those of La_2CuO_4, a simple tight-binding (TB) scheme has been applied to fit the LAPW results of all three compounds. Since the purpose of this analysis is chemical in-

sight rather than quantitative accuracy, a minimal TB basis [involving $Cu(3d)$, $O(2p)$, and $O(2p)$, $Cl(3p)$, or $Br(4p)$ orbitals] has been utilized. This TB model contains a total of 21 parameters for each compound; the fitted values of these TB parameters for $Ca_2CuO_2Cl_2$, $Ca_2CuO_2Br_2$, and La_2CuO_4 are listed in Table I. The resulting TB band structures are illustrated in Fig. 4.

This TB model includes anion-anion interactions over four shells of neighbors. A modified two-center approximation has been introduced to treat the anisotropy of the planar nearest-neighbor O-O interactions.[16] In particular, two distinct $(pp\sigma)$-type parameters $[(pp\sigma)_1^s$ and $(pp\sigma)_1^p]$ are utilized to represent the $O(2p)$-$O(2p)$ interactions between orbitals that form σ and π bonds with neighboring $Cu(3d)$ orbitals. The hybrid parameter, denoted[16] by $(pp\sigma)_1$, is represented by the geometric mean, $[(pp\sigma)_1^s(pp\sigma)_1^p]^{1/2}$. In addition to the three shells of anion-anion interactions that are necessary to introduce c-axis-dispersion effects, it is found that the accuracy of the halo-oxocuprate fits is significantly improved with the introduction of fourth-neighbor planar interactions.

The overall accuracy of this TB fit is evident from a comparison of the TB bands for $Ca_2CuO_2Cl_2$ and $Ca_2CuO_2Br_2$ in Fig. 4 with their LAPW counterparts in Fig. 2. Comparable accuracy is achieved in the La_2CuO_4 fit, though here the rms error (0.23 versus 0.15 eV) is somewhat higher. In the halo-oxocuprates, the largest fitting error (~ 0.5 eV) involves the Δ_1 subband near E_F, whose energy is consistently overestimated by the TB model. An examination of the LAPW wave functions for this state suggests that (omitted) interactions with the unoccupied $Cu(4s)$ states are the source of this discrepancy.

By varying orbital-energy parameters, one can show that the more uniform band distribution in La_2CuO_4
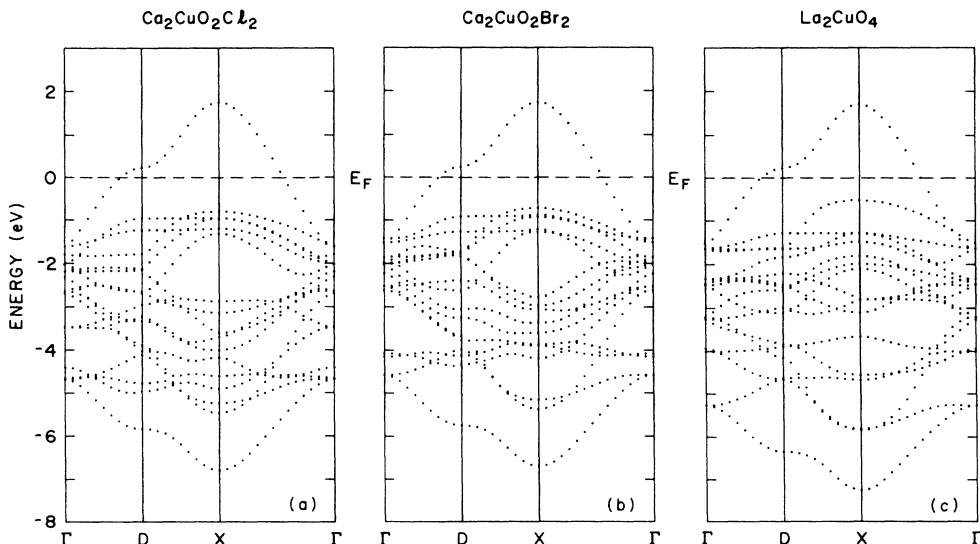

FIG. 4. Tight-binding energy-band results for (a) $Ca_2CuO_2Cl_2$, (b) $Ca_2CuO_2Br_2$, and (c) La_2CuO_4 as determined from the tight-binding parameters of Table I.

(especially near the X point in Fig. 4) is due to the approximate degeneracy of the apical $O(2p)$ and $Cu(3d)$ orbitals. This degeneracy is systematically removed in the halo-oxocuprates by the increased binding energies of the $Br(4p)$ and $Cl(3p)$ orbitals relative to the apical $O(2p)$'s. This is illustrated in Fig. 5, where the crystal-field averaged TB orbital energies of $Ca_2CuO_2Cl_2$, $Ca_2CuO_2Br_2$, and La_2CuO_4 are compared. In each compound, the same approximate energy separation is maintained between $\langle E_d \rangle$ and $\langle E_p \rangle^{planar}$, though both levels shift to higher (~ 0.3 eV) binding energies in La_2CuO_4. This is apparently due to the reduced planar Cu-O bond length (see Table I) and the resulting increase in the overall valence bandwidth in this material. The near degeneracy (~ 0.1 eV) between $\langle E_d \rangle$ and $\langle E_p \rangle^{apical}$ in La_2CuO_4 is systematically increased to ~ 0.5 and ~ 1.3 eV in $Ca_2CuO_2Br_2$ and $Ca_2CuO_2Cl_2$, respectively. Presumably, these chemically induced shifts are important factors which lead to superconductivity in appropriately doped La_2CuO_4 samples but not in the corresponding $Ca_2CuO_2Cl_2$ and $Ca_2CuO_2Br_2$ compounds. These results suggest that it may be necessary to go beyond the usual three-band model[17,18] [which involves only the $Cu\,d\,(x^2-y^2)$ and σ-bonding $O\,p\,(x,y)$ orbitals] in order to investigate theoretically the mechanism for superconductivity in the cuprates.

In summary, we have shown that the calculated band properties of the halo-oxocuprates $Ca_2CuO_2Cl_2$ and $Ca_2CuO_2Br_2$ share the same characteristic half-filled $Cu\,d\,(x^2-y^2)$-$O\,p\,(x,y)$ σ-antibonding subband as the
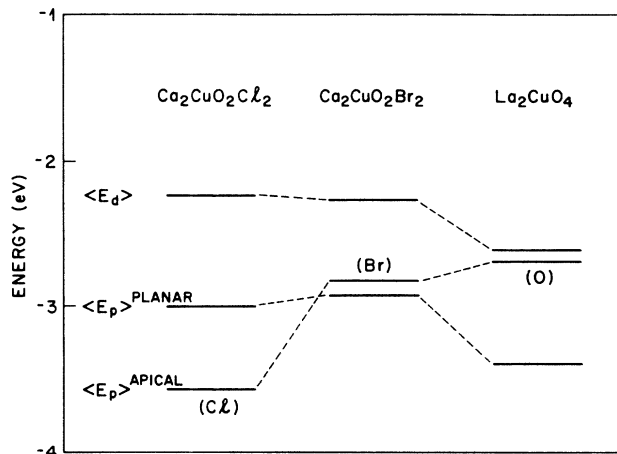

FIG. 5. Comparison of the averaged tight-binding orbital energies $\langle E_a \rangle$ for $Ca_2CuO_2Cl_2$, $Ca_2CuO_2Br_2$, and La_2CuO_4, according to the tight-binding parameters of Table I.

parent compounds of the known cuprate superconductors. Thus far, efforts to induce superconductivity in these materials by altering the band filling within the CuO_2 planes by chemical doping have been unsuccessful. One can conclude that the increased binding energies of the $Cl(3p)$ and $Br(4p)$ states relative to that the apical $O(2p)$ are detrimental to the occurrence of high-temperature superconductivity in the halo-oxocuprates.

[1]B. Grande and H. Müller-Buschbaum, Z. Anorg. Allg. Chem. **417**, 68 (1975); **429**, 88 (1977); **433**, 152 (1977).

[2]J. G. Bednorz and K. A. Müller, Z. Phys. B **64**, 189 (1986).

[3]H. Takagi, S. Uchida, K. Kitazawa, and S. Tanaka, Jpn. J. Appl. Phys. **26**, L123 (1987).

[4]L. F. Mattheiss, Phys. Rev. Lett. **58**, 1028 (1987).

[5]C. Stassis et al., Bull. Am. Phys. Soc. **34**, 428 (1989).

[6]L. L. Miller and D. C. Johnston, Bull. Am. Phys. **34**, 930 (1989); F. C. Chou et al., ibid. **34**, 931 (1989); J. H. Cho et al., ibid. **34**, 931 (1989).

[7]M. K. Wu et al., Phys. Rev. Lett. **58**, 908 (1987).

[8]S. R. Ovshinsky et al., Phys. Rev. Lett. **58**, 2579 (1987).

[9]See, for example, P. K. Davies, et al., Solid State Commun. **64**, 1441 (1987).

[10]J. Kwo et al., Appl. Phys. Lett. **52**, 1625 (1988); P. Marsh et al., Nature (London) **334**, 141 (1988).

[11]A. C. W. P. James, S. M. Zahurak, and D. W. Murphy, Nature (London) **338**, 240 (1989).

[12]L. F. Mattheiss and D. R. Hamann, Phys. Rev. B **33**, 823 (1986).

[13]E. Wigner, Phys. Rev. **46**, 1002 (1934).

[14]A. Fujimori et al., Phys. Rev. B **40**, 7303 (1989).

[15]For a review of the earliest results, see G. Wendin, J. Phys. (Paris) Colloq. **48**, C9-1157 (1987).

[16]L. F. Mattheiss and D. R. Hamann, Phys. Rev. B **40**, 2217 (1989).

[17]C. M. Varma, S. Schmitt-Rink, and E. Abrahams, Solid State Commun. **62**, 681 (1987).

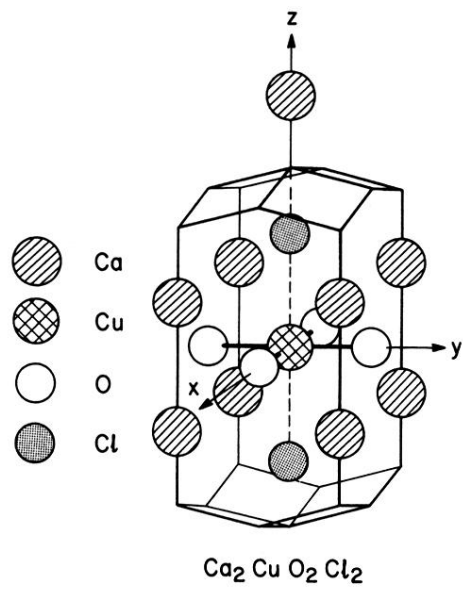[18]V. J. Emery, Phys. Rev. Lett. **58**, 2794 (1987).

$Ca_2 Cu O_2 Cl_2$

FIG. 1. Primitive unit cell for bct $Ca_2CuO_2Cl_2$.